AGU ADVANCING EARTH AND SPACE SCIENCE

Geophysical Research Letters®

RESEARCH LETTER
10.1029/2021GL092885

Key Points:

- Water injection results in early occurrence of the fault seismic slip for both single and cycled injection
- Cycled water injection could reduce both the maximum magnitude of the individual induced seismic events and the total released energy
- Both maximum moment and total energy decrease with an increasing number of water injection cycles

Supporting Information:

Supporting Information may be found in the online version of this article.

Correspondence to:

D. Elsworth and J. B. Zhu,
elsworth@psu.edu;
jbzhu@tju.edu.cn

Citation:

Zhu, J. B., Kang, J. Q., Elsworth, D., Xie, H. P., Ju, Y., & Zhao, J. (2021). Controlling induced earthquake magnitude by cycled fluid injection. *Geophysical Research Letters*, *48*, e2021GL092885. https://doi.org/10.1029/2021GL092885

Received 7 FEB 2021
Accepted 27 AUG 2021

Author Contributions:

Conceptualization: J. B. Zhu, D. Elsworth, H. P. Xie
Data curation: J. Q. Kang
Formal analysis: J. B. Zhu, D. Elsworth, Y. Ju, J. Zhao
Funding acquisition: J. B. Zhu, H. P. Xie, Y. Ju
Investigation: J. Q. Kang
Writing – original draft: J. B. Zhu, J. Q. Kang, D. Elsworth
Writing – review & editing: J. B. Zhu, D. Elsworth, H. P. Xie, Y. Ju, J. Zhao

Controlling Induced Earthquake Magnitude by Cycled Fluid Injection

J. B. Zhu[1,2], J. Q. Kang[2], D. Elsworth[3], H. P. Xie[1], Y. Ju[4], and J. Zhao[5]

[1]Guangdong Provincial Key Laboratory of Deep Earth Sciences and Geothermal Energy Exploitation and Utilization, Shenzhen City Research Institute of Clean Energy, College of Civil and Transportation Engineering, Shenzhen University, Shenzhen, China, [2]State Key Laboratory of Hydraulic Engineering Simulation and Safety, School of Civil Engineering, Tianjin University, Tianjin, China, [3]Energy and Mineral Engineering and Geosciences, G3 Center and EMS Energy Institute, Pennsylvania State University, University Park, State College, PA, USA, [4]State Key Laboratory of Coal Resources and Safe Mining, China University of Mining and Technology, Beijing, China, [5]Department of Civil Engineering, Monash University, Clayton, VIC, Australia

Abstract The possibility of controlling induced earthquake magnitude through managed metering of water injection has yet to be rationalized. Mechanisms of reducing magnitudes of induced events through cycled fluid injection remain unclear. To explore such mechanisms and this possibility, we report experiments with water injection into laboratory faults. Water injection results in early triggering for both single and cycled injection. However, the maximum moment magnitude and total energy of the repeating induced earthquakes during cycled water injection are both lower than those of induced earthquakes induced with continuous injection and for natural earthquakes without water injection. Higher permeability of the host reduces the number of injection-induced earthquakes but increases their moment. With an increasing number of water injection cycles, both maximum moment and total energy decrease, particularly as permeability decreases, while the number of induced events increases. The moment magnitude of induced events can thereby be controlled through cycled fluid injection.

Plain Language Summary Fluid injection-triggered earthquakes have been documented worldwide. Although it is clear that fluid pressure triggers fault slip and results in induced earthquakes, the possibility of controlling induced earthquakes through managed metering of water injection has not been rigorously examined. We performed experiments with single and cycled injection into laboratory faults. Our results show that cycled water injection into a fault could successfully reduce both the maximum magnitude of the individual induced seismic events and the total radiated energy—by setting appropriate water injection schedules. The magnitude and number of induced events are dependent on the number of water injection cycles and rock permeability. These results may provide a better understanding of managing and preventing large induced earthquakes.

1. Introduction

The triggering of fluid injection-induced seismicity has become a key hazard in the recovery of geothermal energy, shale gas, petroleum, and natural gas and in the underground disposal of wastewater (Cornet, 2015; Ellsworth, 2013; Elsworth et al., 2016; McGarr et al., 2015; Weingarten et al., 2015). Fluid disposal induced events have reached M_w 5.8 in (Pawnee) Oklahoma and M_w 5.4 in (Pohang) South Korea for fluid injection in the stimulation of a potential deep geothermal reservoir (Kim et al., 2018; Kroll et al., 2017). These events result from both the injection and the recovery of fluids from the subsurface and are the focus of extensive theoretical, experimental, in situ, and numerical studies (Guglielmi, Cappa, et al., 2015; Moore & Lockner, 2004; Raleigh et al., 1976; Troiano et al., 2013; Yoon et al., 2014). Key features implicated in the triggering involve a change in the pore pressure within the subsurface—this in turn reducing the effective strength of the reservoir or increasing the stress driving failure (Ellsworth, 2013; Kang et al., 2019). Controlling the seismic hazard while simultaneously maintaining normal operations of disposal or energy recovery is a key societal need. Fatigue hydraulic fracturing has been shown to effectively reduce levels of induced seismicity through cycled water injection, and cyclic injections tests on fault stability have been conducted, although mechanisms for improvement remain unclear (Bartlow et al., 2012; Chanard et al., 2019; Noël et al., 2019; Passelègue et al., 2018; Zang et al., 2013; Zhuang et al., 2019). Seismicity may also be reduced by aseismic

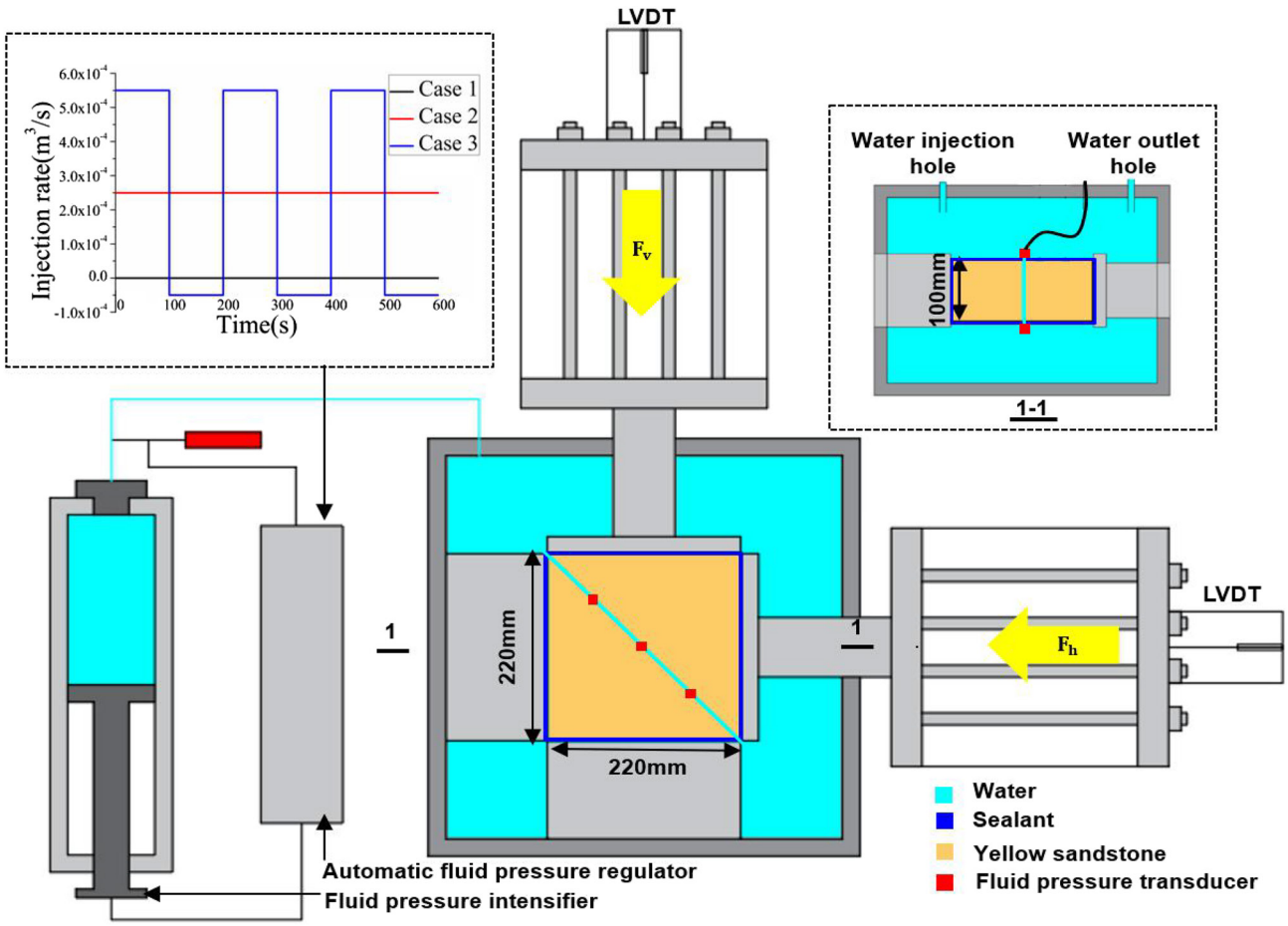

Figure 1. Schematic of biaxial compression experiment on a faulted rock sample with water injection into the fault: electro-hydraulic servo-controlled biaxial compression testing machine loads sample within a pressure cell. Servo-controlled water pressurization system. Linear-variable displacement transducer measure displacements.

deformation driven by the small size of the activated faults, limited extent of activated patches accessed by the pressurization regime (Bourouis & Bernard, 2007; Wei et al., 2015) or by the dependence of slip rate on elevated pore pressure according to rate-state friction laws (Fulton & Rathbun, 2011; Guglielmi, Cappa, et al., 2015). In each case, cyclic fluid injection is one potential mechanism to reduce the magnitude of induced or triggered events by replacing a single large event with multiple cumulative small events. We explore this question in the following, under the pretext of controlling fluid-injection-triggered seismicity but with a potential role in controlling tectonic earthquakes.

2. Materials and Methods

2.1. Apparatus and Samples

An electro-hydraulic servo-controlled biaxial compression testing machine is used to load prismatic samples containing an angled laboratory fault (Figure 1). The prismatic samples are saw-cut along the diagonal to represent a laboratory fault. These fault surfaces are polished with #150 grit grinding compound (~100 μm abrasive size) to create reproducible surfaces and eliminate the potentially uncontrolled influence of fault surface roughness on stress drop. The diagonally fractured samples are confined in a sealed steel pressure cell with servo-controlled rate of injection of water, as shown in Figure 1. Prismatic samples ($220 \times 220 \times 100$ mm^3) are prepared from sandstone (Changsha, China) with permeabilities of $1.1e^{-18}$ m^2 (sample A), $7.7e^{-17}$ m^2 (sample B), and $3.3e^{-16}$ m^2 (sample C) representing varied sensitivities to injection rate. The permeability is measured on rock samples from the same rock blocks at an effective stress of 8 MPa

using an ultra-low permeability tester. All external surfaces of the sample are sealed with high-strength sealant to guarantee seepage only into and along the fault (Figure 1) and the sample is placed within the pressure cell.

2.2. Loading and Water Injection Condition

The cell is water-filled and maintained at atmospheric pressure (0 MPa) while equal horizontal and vertical stresses are applied to the saturated sample ($F_h = F_v = 8$ MPa). Subsequently, F_h is fixed while F_v is increased by applying a displacement rate of 0.02 mm/s. At the same time, water is injected into the pressure cell and the pore pressure increases on the exterior of the unsealed fault within the prismatic block. In addition to one case without water injection (Case 1), seven other injection schedules match the same total injected volume over the same total duration (600s) but with intervening pauses in injection. These seven schedules include one case of continuous water injection at an injection rate of 2.5×10^{-4} m^3/s (Case 2) and six schedules of cycled water injection with varied injection-quiescence period for 3 cycles (100s of injection separated by 100s of quiescence; i.e., 100s:100s) (Case 3); for 6 cycles (50s:50s) (Case 4); for 12 cycles (25s:25s) (Case 5); for 24 cycles (12.5s:12.5s) (Case 6); for 48 cycles (6.25s:6.25s) (Case 7); and for 96 cycles of (3.125s:3.125s) (Case 8). During the cycled water injections, the injection rate ($q = 5.5 \times 10^{-4}$ m^3/s) is approximately double that of the continuous injection case and negligible ($q = -0.5 \times 10^{-4}$ m^3/s) during the quiescence period. Water pressure on the laboratory fault is monitored using six precision pressure transducers fixed near the fault (red dots in Figure 1). The water pressures monitored by those six transducers are uniform. The shear stress and the effective normal stress on the fault are calculated as:

$$\tau = \frac{\sigma_1 - \sigma_3}{2} \sin 2\theta \tag{1}$$

$$\sigma_n^{'} = \frac{\sigma_1 + \sigma_3 - P_f}{2} - \frac{\sigma_1 - \sigma_3}{2} \cos 2\theta \tag{2}$$

where τ and $\sigma_n^{'}$ are the shear stress and the effective normal stress, respectively; σ_1 and σ_3 are the vertical and horizontal stresses, respectively; θ is the angle between the vertical stress and the fault plane, and P_f is the water pressure.

The total vertical displacement is measured using the external linear-variable displacement transducer (LVDT). Evolving fault slip is calculated from the total vertical displacement minus deformation of the loading frame and the rock matrix, as:

$$d = \frac{d_{LVDT} - d_1 - d_2}{\cos\theta} \tag{3}$$

where d is the fault-parallel slip, d_1 and d_2 are the deformation of the loading bar and the rock matrix, respectively and magnitudes are corrected for the inclination of the fault relative to the vertical loading axis θ.

The criterion for fault activation is:

$$\frac{\tau}{\sigma_n^{'}} = \mu_0 \tag{4}$$

where is μ_0 the static friction coefficient of the angled laboratory fault and obtained from laboratory shear testing. The static friction coefficients of the fault of Samples A, B, and C are broadly consistent at 0.30, 0.29, and 0.31, respectively.

2.3. Total Seismic Energy and Moment Magnitude

Since the laboratory fault is planar, the total radiated seismic energy is the difference between the elastic strain energy and the energy consumed as frictional heat, where the fracture energy is negligible for such simple case (Abercrombie & Rice, 2005; Scholz, 2002). During loading and water injection, the stress and deformation of the sample and the water pressure along the fault are monitored and recorded. The effective shear stress and evolving shear displacement along the fault are recovered with three repeats of each experiments conducted and averaged results reported here. We used shear stress drop, fault area and incremental fault slip (see Figure 2) to calculate the total radiated seismic energy and the moment magnitude (M_w) of

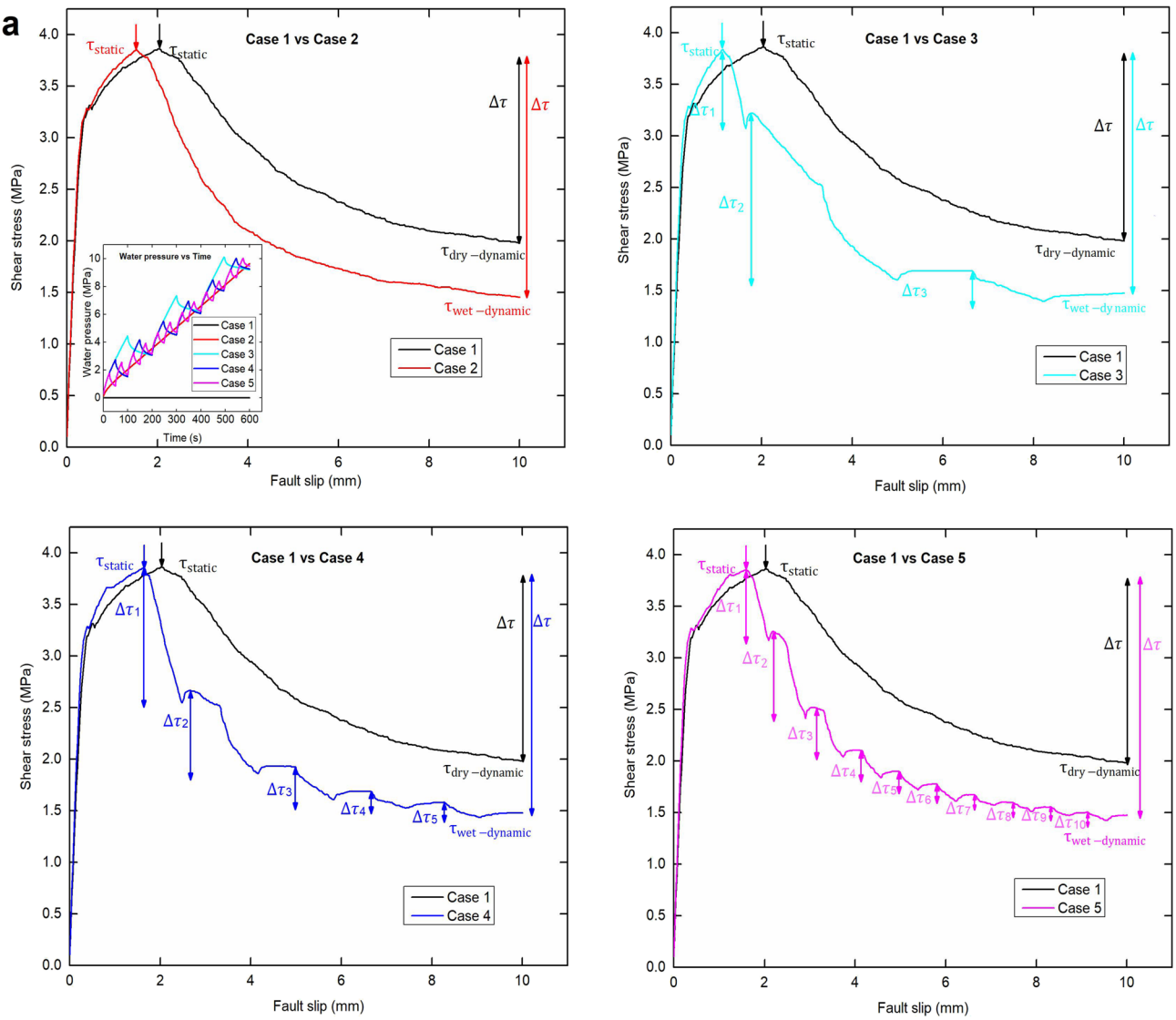

Figure 2. Fault slip behavior of Samples A, B, and C for water injection Cases 1, 2, 3, 4, and 5: shear stress versus fault slip of samples (a) A; (b) B; (c) (C) Cases 1–5 refer to no water injection (Case 1), continuous water injection (Case 2), water injection for 3 cycles (Case 3), water injection for 6 cycles (Case 4), and water injection for 12 cycles (Case 5), respectively, where the total volume of water injected is the same in all cases (Cases 2–5). Changes in water pressure within the laboratory fault as a function of time for all cases are also illustrated. Each unstable slip is marked as $\Delta\tau_i$ (i = 1, 2, 3...).

the slip events for each water injection schedule with the following equations (Abercrombie & Rice, 2005; McGarr, 2012; Scholz, 2002):

$$E_s = \tau_a \Delta d A \tag{5}$$

$$\log_{10} E_s = 1.5 M_w + 4.8 \tag{6}$$

where E_s is the total radiated seismic energy, τ_a is the apparent stress and equal to a quarter of the stress drop, Δd is the incremental fault slip, and A is the fault area.

3. Results

3.1. Stress Drops

We report biaxial compression tests on laboratory faults coupled with cyclic water injection (see Figure 1) to define controlling impacts of injection rates and permeability of the host on the size and frequency of

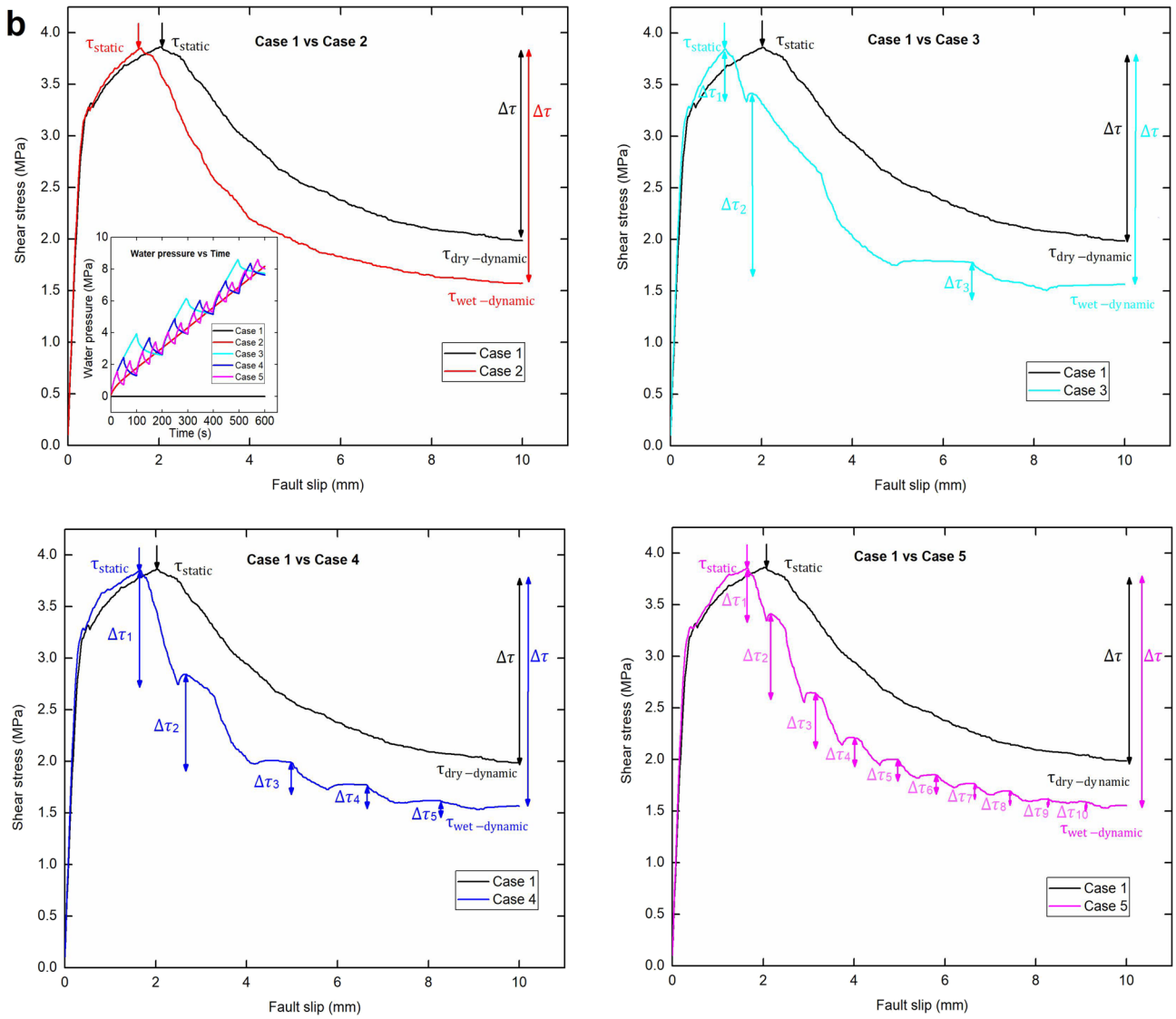

Figure 2. *Continued.*

repeating induced earthquakes. The resulting fault slip behavior is shown to be strongly dependent on the water injection schedule. Notably, in all cases, the total injection volume into the cell is identical. Figure 2 shows the fault slip behavior of the low (A), moderate (B), and high (C) permeability samples without water injection (Figure 1) in Case 1, with continuous constant-rate injection in Case 2 and cycled injections at an approximately doubled-rate (Figure 1) in Cases 3 (200s), 4 (100s), and 5 (50s). For Case 3, the cycle time is 100s of approximately double-rate continuous injection ($q = 5.5 \times 10^{-4}$ m^3/s) followed by 100s with almost no injection ($q = -5 \times 10^{-5}$ m^3/s) for a composite full injection-quiescence period of 200s, and similarly for Cases 4 (100s) and 5 (50s). The injection rate for the cycled injections results in the same net injection volume with time for all cases. In Cases 1 and 2, the slip of Samples A, B, and C exhibit stick-slip behavior. In Cases 3, 4, and 5, aseismic slip and stick-slip events occur for Samples A, B, and C (Leeman et al., 2016; Tinti et al., 2016; Wu & McLaskey, 2019). Compared to the fault slip for Case 1 without water injection, slip occurred earlier for all cases with water injection–driven by the more rapid reduction in effective stress and related strength of the fault as tectonic driving stresses build at the same rate. A single stress drop occurred when either no water was injected (Case 1) or when injection was continuous (Case 2), with the stress drop for continuous injection (Case 2) both larger and earlier than that for no injection (Case 1). For three cycles of injection (200s; Case 3), three stress drops were observed for the lower permeability samples (A and B)

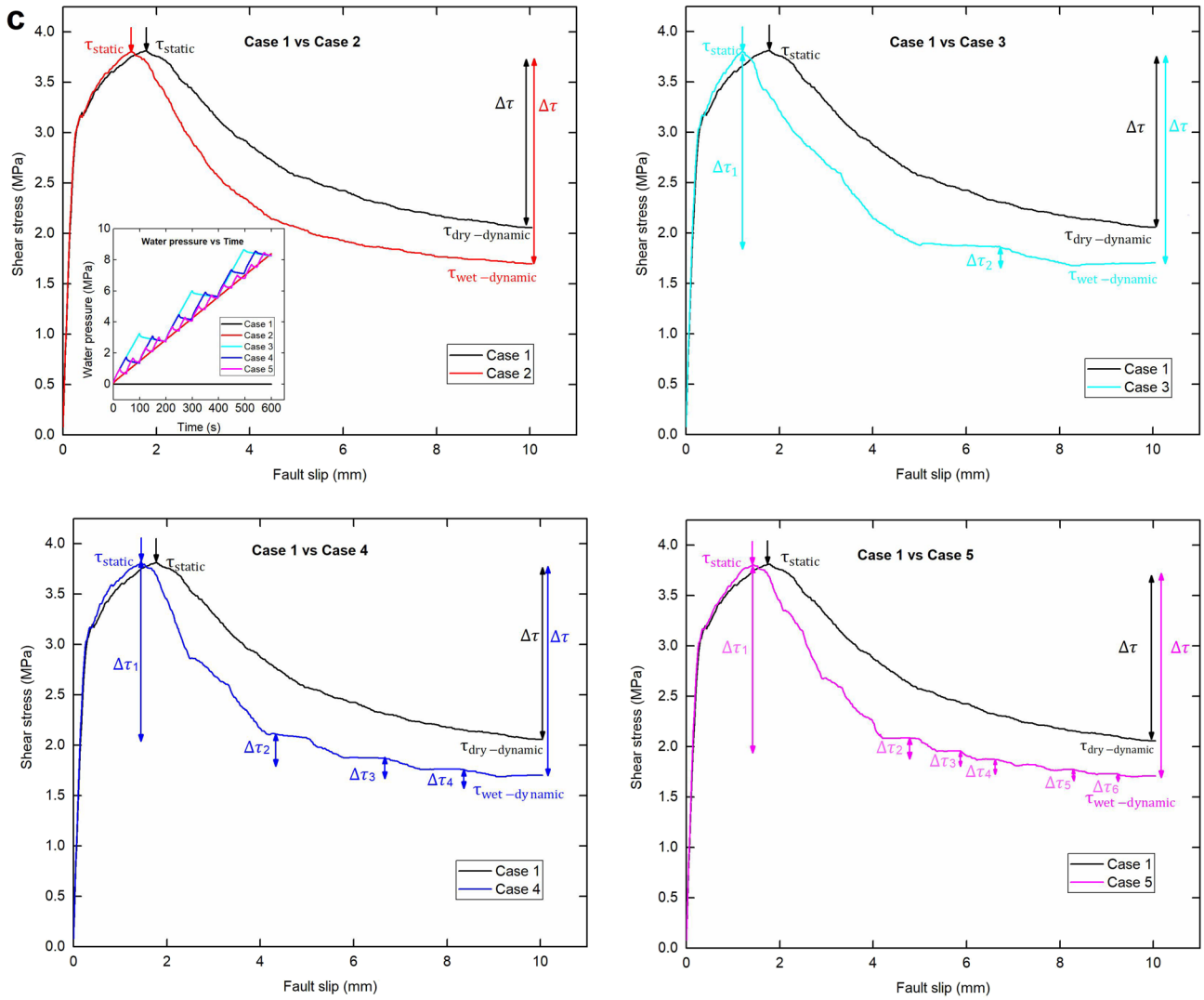

Figure 2. *Continued.*

and two stress drops for the highest permeability sample (Sample C); each of these individual stress drops was smaller than that for the cases without water injection (Case 1) and with continuous water injection (Case 2). For Case 4, with six water injection cycles of 100s, five stress drops were observed for the lowest permeability samples (Samples A and B), while four stress drops were observed for the highest permeability (Sample C); again, each of these stress drops was smaller than those for either no injection or continuous injection (Cases 1 and 2). For 12 water injection cycles of 50s (Case 5), a total of 10 stress drops were observed for the low permeability samples (A and B), while six stress drops were observed for the highest permeability sample (C); again, each of these stress drops was individually smaller than that for either no- or continuous-injection (Cases 1 and 2).

3.2. Earthquake Moment Magnitude

Figure 3 shows the total radiated seismic energy and the moment magnitude (M_w) of the slip events for each water injection schedule. For low permeability (A), the number of slip events coincide with the number of shear stress drops, which increases with an increasing number of water injection cycles. Only a single large slip event occurs for both no injection (Case 1) and continuous water injection (Case 2). The moment magnitude and total energy are less for continuous injection (Case 2) than for no injection (Case 1)—

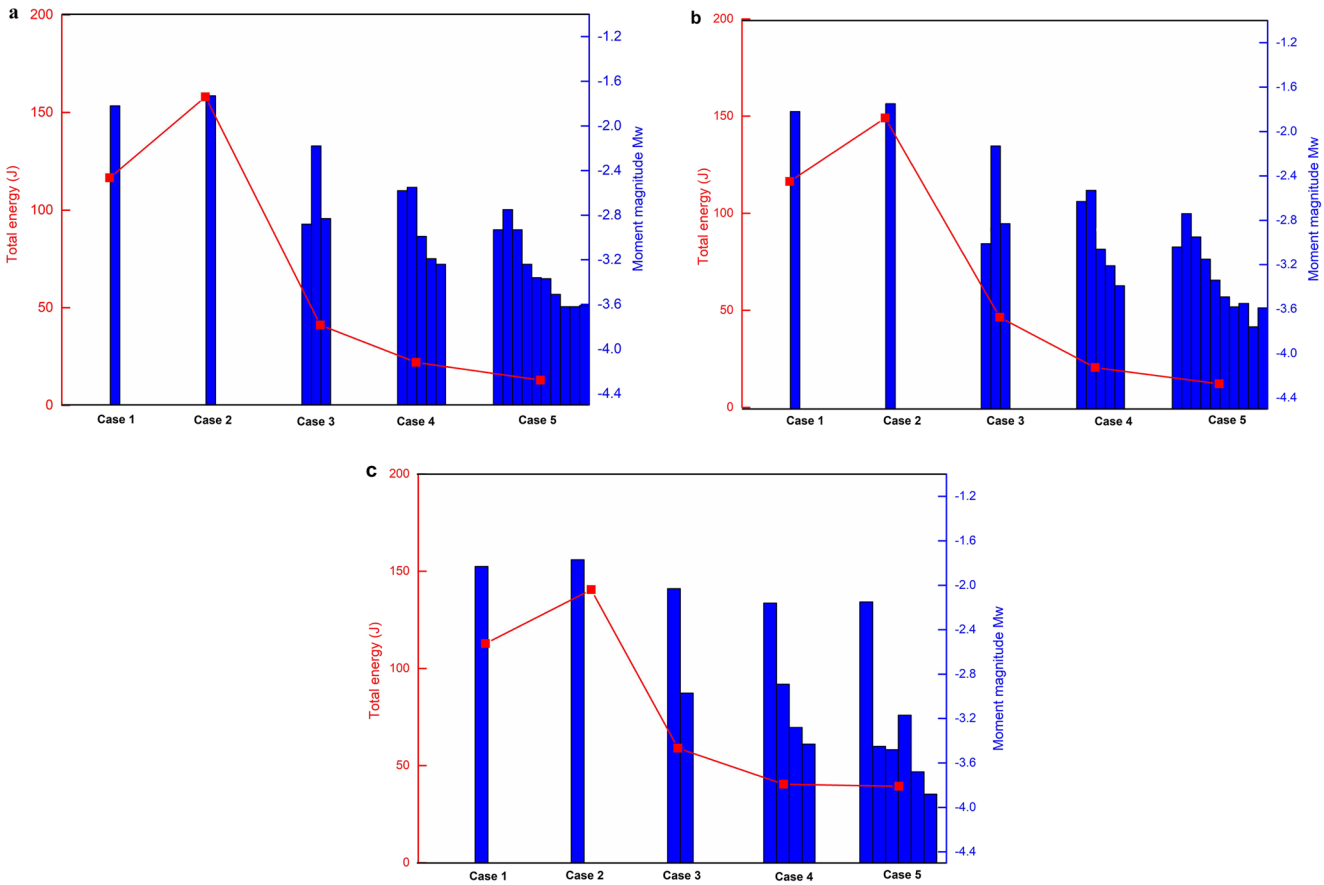

Figure 3. Total seismic energy and moment magnitudes (M_w) of events distributed among the various water injection cases: (a) Sample A; (b) Sample B; (c) Sample (c) Cases 1–5 refer to no water injection (1), continuous water injection (2), water injection split over 3 cycles (3), water injection split over 6 cycles (4), and water injection split over 12 cycles (5), respectively. Total injected water volume identical in all cases (2–5).

presumably because failure is prematurely triggered before a large tectonic stress can build. Compared with the results for no injection (Case 1), the reduction in the total seismic energy for cyclic injection periodicities of 200s (Case 3), 100s (Case 4), and 50s (Case 5) were 65%, 81%, and 89%, respectively, with maximum moment magnitudes decreasing by 20%, 40%, and 51%, respectively. Comparing with the results for continuous injection (Case 2), the reduction in the total seismic energy for cyclic injection periodicities of 200s (Case 3), 100s (Case 4), and 50s (Case 5) were 74%, 86%, and 92%, respectively, with maximum moment magnitudes decreasing by 26%, 47%, and 59%, respectively. All injection schedules result in the same volume of injected water into the functionally incompressible system. We conclude that compared with both natural tectonic earthquakes that occur absent water injection and triggered earthquakes that occur as a result of continuous water injection, maximum moment magnitude and total radiated energy during cyclic-injection triggered events are uniformly lower and decrease with an increase in the number of repeated cycles—for the same volume injected and average injection rate. The findings for the higher permeability samples (B and C) are the same as those for low permeability (sample A) except for the magnitude of the reduction in energy release—which is a greater reduction for the low permeability samples.

3.3. Relation Between Earthquake Magnitude and Injection Cycles

Figure 4 shows the dependence of the number and the maximum moment magnitude of injection-induced earthquakes on the number of water injection cycles. In all instances, the total injected volume, loading rates and durations of the injection are identical. With an increasing number of water injection cycles, the number of induced events increases while the maximum moment magnitude and total energy of the induced earthquakes both decrease. The number of events scaled between 1:1 and 1:2 with the number of

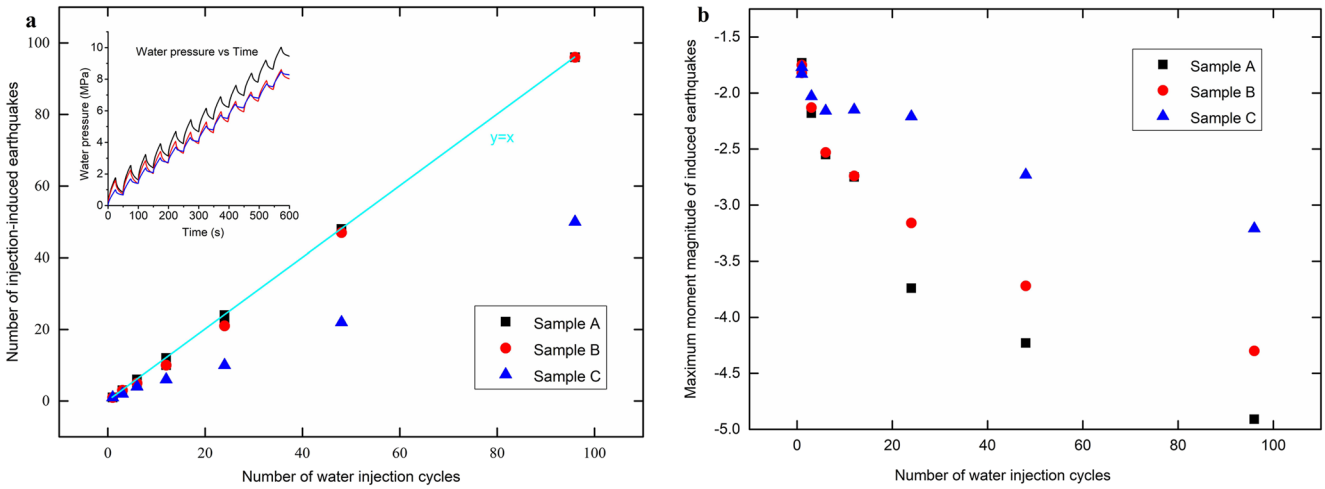

Figure 4. Dependence of the number and the maximum moment magnitude of injection-induced earthquakes on the number of water injection cycles, for which the total injected water volume and the duration of water injection are identical: (a) number of injection-induced earthquakes versus the number of water injection cycles for Samples A, B, and C; (b) maximum moment magnitude of induced earthquakes versus the number of water injection cycles.

injection cycles–identifying that each pressurization cycle is able to trigger a single event in the low-permeability rock.

4. Discussion

Water injection into a fault may prematurely trigger fault failure before such an event would naturally occur. This is because fault failure will occur earlier when water is injected into a fault relative to the case of no injection if all other loading conditions are equivalent (Ellsworth, 2013). Figure S1 shows the time (t_0) of initial fault failure of Samples A, B, and C for all cases. Compared with Case 1 without water injection, t_0 for Cases 2, 3, 4, and 5 with water injection are earlier, indicating early fault failure when water is injected. This is a result of reduced effective stresses reducing the shear strength. In contrast to Case 2 for continuous water injection, t_0 for Cases 3, 4, and 5 with cycled water injection are smaller, indicating early fault failure occurs when water is cyclically injected, resulting from the higher pressurization rate relative to that for continuous injection (Figure 2).

The locus of peaks in shear stress for cycled pressurization (Figure S1) form a plateau slightly higher than the friction coefficient—representing the partial incursion of fluid into the fault—with part of the fault likely under-pressured. This horizontal locus of peaks represents a balance between the tectonic loading of the fault and the pressurization rate of the fault. This reactivation plateau is higher and the peaks earlier for the low permeability samples A and B relative to the highest permeability sample C. The high permeability promotes leak-off within the sample and reduces the effective pressurization rate of the fault while allowing the fault to be more fully infiltrated, delaying reactivation as the pressure builds to a peak.

Heat will be generated during seismic fault slip (Rice, 2017). Attributed to the interaction between frictional heat and water pressure (the wet stick-slip model), the wet dynamic frictional strength after water injection is lower than the dry dynamic frictional strength without water injection. Hence, the one-time stress drop due to continuous water injection and the total stress drop due to cyclic water injections are both larger than those without water injection.

Compared with both natural tectonic earthquakes that occur absent water injection and triggered earthquakes that occur as a result of continuous water injection, maximum moment magnitude and total radiated energy during cyclic-injection triggered events are uniformly lower. Both aseismic and seismic fault slip are triggered by fluid pressurization with aseismic deformation potentially culminating in a seismic event (Guglielmi, Cappa, et al., 2015; Scuderi & Collettini, 2016). During cyclic water injection, the water pressure in the fault does not reach steady-state and therefore it increases only intermittently between pressure drops (Figure 2) before being elevated by the onset of the next injection/pressurization cycle. An increase in water

pressure facilitates seismic fault slip but the following decrease in pressure may strengthen the fault and reinitiate aseismic fault slip (Scholz, 2002; Sibson, 1973) and shear stress redistribution. This is one potential reason why cyclic injection results in multiple aseismic slips, triggering a larger number of small earthquakes instead of a single large event. In addition, with an increasing number of water injection cycles but with identical total injection volumes and average injection rates, more small earthquakes are triggered, and hence, the maximum moment magnitude and total energy of the induced earthquakes must both decrease.

The number of events resulting from cycled injection increases with decreasing rock permeability. The number of injection-triggered slip events is similar to the number of water injection cycles for low permeability but is less than the number of water injection cycles for high permeability. This is consistent with reducing fault pressure, through leakoff, and delaying the onset of failure by increasing the time taken to reach a critical combination of high fault shear stress and fluid overpressure—each driven at different rates. In addition, the maximum moment magnitude of the injection-triggered earthquakes decreases with decreasing rock permeability. This is because a higher water pressure is induced along the fault where rock permeability is lowest (e.g., Sample A in Figure 4a)—fluid mass loss into the surrounding rock matrix is staunched. Low permeability fault-adjacent rocks (e.g., Sample A) allow a greater increase in the water pressure within the fault (due to both water injection and external loading) and decrease in the water pressure along a fault during fault slip, resulting in a greater increase then decrease of the critical stiffness of the fault, respectively. This change in fault stiffness potentially triggers a distinct switch between fault seismic (the critical stiffness of the fault is larger than the stiffness of the surrounding rock) and aseismic slip behaviors (the critical stiffness of the fault is smaller than the stiffness of the surrounding rock) (Alghannam & Juanes, 2020). In addition, secondary damage is observed in the host during fault rupture (see Figure S2), forming a damage zone that enhances the permeability of the surrounding rock, further lowering water pressure within the fault. This potentially leads to a decrease of the critical stiffness of the fault (Alghannam & Juanes, 2020) and drives aseismic fault slip (Guglielmi, Cappa, et al., 2015; Guglielmi, Elsworth, et al., 2015; Zhu & Kang, 2020). Therefore, the potential for the occurrence of large injection-triggered (or natural) earthquakes may potentially be reduced via cycled water injection by inducing a number of small earthquakes, particularly in rocks with a low permeability, such as granite, limestone and shale.

Fault slip is a complex process and is shown to be dependent on a number of factors, including fault type and stress conditions. However, the observations and their interpretation, described in this paper, provide preliminary evidence of the feasibility of controlling the moment magnitude of induced (or possibly natural) events through cycled water injection. By setting appropriate water injection schedules, cycled water injection into a fault could successfully reduce both the maximum magnitude of the individual induced seismic events and the total radiated energy.

5. Conclusions

Our laboratory findings about earthquakes induced by fluid injection have highlighted several points.

1. Water injection into fault results in early occurrence of the fault seismic slip.
2. Compared with the natural earthquake without water injection, the moment magnitude of the single induced earthquake during continuous water injection is larger, while the maximum moment magnitude and total energy of the induced earthquakes during cyclic water injection are both lower.
3. With increasing water injection cycles of identical total injection volume and injection rate, both the maximum moment magnitude and total energy of induced earthquake both decrease while the number of induced earthquakes increases.
4. The effect of cyclic water injection on reducing the earthquakes becomes more significant with decreasing rock permeability.

Conflict of Interest

The authors declare no conflicts of interest relevant to this study.

Data Availability Statement

Data for Figures can be found at https://doi.org/10.6084/m9.figshare.16569642.v1 (Figure 1 has no data).

Acknowledgments
This work is funded by the Program for Guangdong Introducing Innovative and Entrepreneurial Teams under award 2019ZT08G315 and the National Science Foundation of China under awards 51974197 and 51727807.

References

Abercrombie, R. E., & Rice, J. R. (2005). Can observations of earthquake scaling constrain slip weakening? *Geophysical Journal International*, *162*, 406–424. https://doi.org/10.1111/j.1365-246x.2005.02579.x

Alghannam, M., & Juanes, R. (2020). Understanding rate effects in injection-induced earthquakes. *Nature Communications*, *11*, 3053. https://doi.org/10.1038/s41467-020-16860-y

Bartlow, N. M., Lockner, D. A., & Beeler, N. M. (2012). Laboratory triggering of stick-slip events by oscillatory loading in the presence of pore fluid with implications for physics of tectonic tremor. *Journal of Geophysical Research*, *117*, B11411. https://doi.org/10.1029/2012jb009452

Bourouis, S., & Bernard, P. (2007). Evidence for coupled seismic and aseismic fault slip during water injection in the geothermal site of Soultz (France), and implications for seismogenic transients. *Geophysical Journal International*, *169*, 723–732. https://doi.org/10.1111/j.1365-246x.2006.03325.x

Chanard, K., Nicolas, A., Hatano, T., Petrelis, F., Latour, S., Vinciguerra, S., & Schubnel, A. (2019). Sensitivity of acoustic emission triggering to small pore pressure cycling perturbations during brittle creep. *Geophysical Research Letters*, *46*, 7414–7423. https://doi.org/10.1029/2019gl082093

Cornet, F. H. (2015). Earthquakes induced by fluid injections. *Science*, *348*, 1204–1205. https://doi.org/10.1126/science.aab3820

Ellsworth, W. L. (2013). Injection-induced earthquakes. *Science*, *341*, 1225942. https://doi.org/10.1126/science.1225942

Elsworth, D., Spiers, C. J., & Niemeijer, A. R. (2016). Understanding induced seismicity. *Science*, *354*, 1380–1381. https://doi.org/10.1126/science.aal2584

Fulton, P. M., & Rathbun, A. P. (2011). Experimental constraints on energy partitioning during stick-slip and stable sliding within analog fault gouge. *Earth and Planet Science Letter*, *308*, 155–192. https://doi.org/10.1016/j.epsl.2011.05.051

Guglielmi, Y., Cappa, F., Avouac, J. P., Henry, P., & Elsworth, D. (2015). Seismicity triggered by fluid injection-induced aseismic slip. *Science*, *348*, 1224–1226. https://doi.org/10.1126/science.aab0476

Guglielmi, Y., Elsworth, D., Cappa, F., Henry, P., Gout, C., Dick, P., & Durand, J. (2015). In situ observations on the coupling between hydraulic diffusivity and displacements during fault reactivation in shales. *Journal of Geophysical Research: Solid Earth*, *120*, 7729–7748. https://doi.org/10.1002/2015jb012158

Kang, J. Q., Zhu, J. B., & Zhao, J. (2019). A review of mechanisms of induced earthquakes: From a view of rock mechanics. *Geomechanics and Geophysics for Geo-Energy and Geo-Resources*, *5*(3), 171–196. https://doi.org/10.1007/s40948-018-00102-z

Kim, K. H., Ree, J. H., Kim, Y. H., Kim, S., Kang, S. Y., & Seo, W. (2018). Assessing whether the 2017 Mw 5.4 Pohang earthquake in South Korea was an induced event. *Science*, *360*, 1007–1009. https://doi.org/10.1126/science.aat6081

Kroll, K. A., Cochran, E. S., & Murray, K. E. (2017). Poroelastic properties of the Arbuckle Group in Oklahoma derived from well fluid level response to the 3 September 2016 Mw 5.8 Pawnee and 7 November 2016 Mw 5.0 Cushing Earthquakes. *Seismological Research Letters*, *88*, 963–970. https://doi.org/10.1785/0220160228

Leeman, J. R., Saffer, D. M., Scuderi, M. M., & Marone, C. (2016). Laboratory observations of slow earthquakes and the spectrum of tectonic fault slip modes. *Nature Communications*, *7*, 11104. https://doi.org/10.1038/ncomms11104

McGarr, A. (2012). Relating stick-slip friction experiments to earthquake source parameters. *Geophysical Research Letters*, *39*, L05303. https://doi.org/10.1029/2011gl050327

McGarr, A., Bekins, B., Burkardt, N., Dewey, J., Earle, P., Ellsworth, W., et al. (2015). Coping with earthquakes induced by fluid injection. *Science*, *347*, 830–831. https://doi.org/10.1126/science.aaa0494

Moore, D. E., & Lockner, D. A. (2004). Crystallographic controls on the frictional behavior of dry and water-saturated sheet structure minerals. *Journal of Geophysical Research*, *109*, B03401. https://doi.org/10.1029/2003jb002582

Noël, C., Passelègue, F. X., Giorgetti, C., & Violay, M. (2019). Fault reactivation during fluid pressure oscillations: Transition from stable to unstable slip. *Journal of Geophysical Research: Solid Earth*, *124*, 10940–10953. https://doi.org/10.1029/2019jb018517

Passelègue, F. X., Brantut, N., & Mitchell, T. M. (2018). Fault reactivation by fluid injection: Controls from stress state and injection rate. *Geophysical Research Letters*, *45*(12), 837–846. https://doi.org/10.1029/2018gl080470

Raleigh, C. B., Healy, J. H., & Bredehoeft, J. D. (1976). An experiment in earthquake control at Rangely, Colorado. *Science*, *191*, 1230–1237. https://doi.org/10.1126/science.191.4233.1230

Rice, J. R. (2017). Heating, weakening and shear localization in earthquake rupture. *Philosophical Transactions of The Royal Society: A Mathematical Physical and Engineering Sciences*, *375*. https://doi.org/10.1098/rsta.2016.0015

Scholz, C. H. (2002). *The mechanics of earthquakes and faulting*: Cambridge University Press.

Scuderi, M. M., & Collettini, C. (2016). The role of fluid pressure in induced vs. triggered seismicity: Insights from rock deformation experiments on carbonates. *Scientific Reports*, *6*, 24852. https://doi.org/10.1038/srep24852

Sibson, R. (1973). Interactions between temperature and pore-fluid pressure during earthquake faulting and a mechanism for partial or total stress relief. *Nature*, *243*, 66–68. https://doi.org/10.1038/physci243066a0

Tinti, E., Scuderi, M. M., Scognamiglio, L., Stefano, G. D., Marone, C., & Collettini, C. (2016). On the evolution of elastic properties during laboratory stick-slip experiments spanning the transition from slow slip to dynamic rupture. *Journal of Geophysical Research: Solid Earth*, *121*, 8569–8594. https://doi.org/10.1002/2016jb013545

Troiano, A., Di Giuseppe, M. G., Troise, C., Tramelli, A., & De Natale, G. A. (2013). Coulomb stress model for induced seismicity distribution due to fluid injection and withdrawal in deep boreholes. *Geophysical Journal International*, *195*, 504–512. https://doi.org/10.1093/gji/ggt229

Wei, S., Avouac, J.-P., Hudnut, K. W., Donnellan, A., Parker, J. W., Graves, R. W., et al. (2015). The 2012 Brawley swarm triggered by injection-induced aseismic slip. *Earth and Planet Science Letter*, *422*, 115–125. https://doi.org/10.1016/j.epsl.2015.03.054

Weingarten, M., Ge, S., Godt, J. W., Bekins, B. A., & Rubinstein, J. L. (2015). High-rate injection is associated with the increase in U.S. mid-continent seismicity. *Science*, *348*, 1336–1340. https://doi.org/10.1126/science.aab1345

Wu, B. S., & McLaskey, G. C. (2019). Contained laboratory earthquakes ranging from slow to fast. *Journal of Geophysical Research: Solid Earth*, *124*, 10270–10291. https://doi.org/10.1029/2019jb017865

Yoon, J. S., Zang, A., & Stephansson, O. (2014). Numerical investigation on optimized stimulation of intact and naturally fractured deep geothermal reservoirs using hydro-mechanical coupled discrete particles joints model. *Geothermics*, *52*, 165–184. https://doi.org/10.1016/j.geothermics.2014.01.009

Zang, A., Yoon, J. S., Stephansson, O., & Heidbach, O. (2013). Fatigue hydraulic fracturing by cyclic reservoir treatment enhances permeability and reduces induced seismicity. *Geophysical Journal International*, *195*, 1282–1287. https://doi.org/10.1093/gji/ggt301

Zhu, J. B., & Kang, J. Q. (2020). Fluid injection-induced seismicity considering secondary damage and heterogeneity in the surrounding rock. *Bulletin of Engineering Geology and the Environment*, *79*, 2635–2646. https://doi.org/10.1007/s10064-019-01676-y

Zhuang, L., Kim, K. Y., Jung, S. G., Diaz, M., Min, K. B., Zang, A., et al. (2019). Cyclic hydraulic fracturing of pocheon granite cores and its impact on breakdown pressure, acoustic emission amplitudes and injectivity. *International Journal of Rock Mechanics and Mining Sciences*, *122*, 104065. https://doi.org/10.1016/j.ijrmms.2019.104065